Resonant Raman scattering in an InSb/$In_{1-x}Al_xSb$ strained-layer superlattice and in $In_{1-x}Al_xSb$ epilayers on InSb

V. P. Gnezdilov,* D. J. Lockwood, and J. B. Webb
Institute for Microstructural Sciences, National Research Council, Ottawa, Ontario, Canada K1A 0R6
(Received 29 March 1993; revised manuscript received 6 July 1993)

Resonant Raman scattering was used to study an InSb/$In_{1-x}Al_xSb$ strained-layer superlattice and the InSb and $In_{1-x}Al_xSb$ parent materials. Resonant enhancement peaks were observed in epilayer films in the regions of the E_1 and $E_1+\Delta_1$ optical gaps. In the superlattice, two sets of peaks observed in the plots of the Raman cross section versus exciting photon energy are shown to originate from the independent electronic transitions in the alternating layers. The calculated resonance Raman profiles for two phonons in the alloy layers are in reasonable agreement with experiment. Estimates of the strain and confinement effects in these layers were made and these agree with the observed differences from the parent materials.

I. INTRODUCTION

In recent years considerable theoretical and experimental interest has been focused on semiconductor superlattices. In these investigations, Raman and, in particular, resonant Raman spectroscopy has played a significant role. This method allows one to obtain, for example, information on the superlattice vibrational properties, on the crystalline quality, on the strain within the superlattice layers, and on special kinds of ordering within alloy layers. Resonant Raman scattering (RRS) from phonons is useful for obtaining information on electronic states of superlattices.[1] Although this method does not allow for exact determination of transition energies, it provides information on whether the electronic states under study are confined within the quantum wells or if they extend through the whole structure. This possibility is due to the exploitation of the modulation produced in the electronic states by the optical lattice vibrations that are characteristic of each type of layer and that are not significantly affected by the periodicity of the superlattice.[2,3]

Most of the previous RRS work was performed on direct band-gap materials in the vicinity of the Brillouin-zone center and the most thoroughly studied system in the past few years has been GaAs/$Ga_{1-x}Al_xAs$ heterostructures.[4] Unfortunately, there is limited experimental information about the interband transitions in superlattices away from the center of the Brillouin zone. The first observations of the interband transitions in superlattices at different points of the Brillouin zone were made with the electroreflectance method:[5,6] the $\bar{E}_1$, $\bar{E}_1+\bar{\Delta}_1$, and $\bar{E}_2$ electronic transitions were observed in the electroreflectance spectrum of GaAs/$Ga_{1-x}Al_xAs$ superlattices,[5] and two sets of electronic structures associated with GaSb and AlSb layers in a GaSb/AlSb superlattice were found.[6] Hence, in the latter case, it was observed that there were two bands of E_1 transitions confined in alternating layers. Only two investigations of Raman resonances at the E_1 gap of zinc-blende superlattices are known.[7,8] In these studies the resonant behavior of the longitudinal-optical (LO) phonons of only one of the two alternating layers was analyzed.

The aim of this work was to perform an analysis of the electronic structure of an InSb/$In_{0.561}Al_{0.439}Sb$ superlattice in the region of the E_1 and $E_1+\Delta_1$ electronic transitions of the host materials using the resonant Raman scattering method. Epitaxial InSb and $In_{0.56}Al_{0.44}Sb$ films have also been probed by the Raman method, since information regarding InSb-based alloys is very limited, to reveal the influence of the superlattice effect.

The outline of this paper is as follows. In Sec. II the experimental details are given and in Sec. III the results obtained for epilayer films and superlattice are presented and discussed. A summary and conclusions are given in the final section.

II. EXPERIMENTAL SETUP AND PROCEDURE

Three samples grown by magnetron sputter epitaxy on (001)InSb substrates[9,10] were analyzed: (i) InSb single epilayer film. (ii) $In_{0.56}Al_{0.44}Sb$ single epilayer film. The layer thickness of both films was ~ 0.4 μm. The $In_{0.56}Al_{0.44}Sb$ film showed surface defect lines under optical phase contrast microscopy indicating strain relaxation had occurred through misfit dislocation formation. (iii) InSb/$In_{0.561}Al_{0.439}Sb$ 20-period strained-layer superlattice. The InSb and alloy layer thicknesses were 72.5 and 41.0 Å, respectively. An x-ray and Raman scattering analysis showed[9,10] that the superlattice was of excellent epitaxial quality.

The Raman scattering measurements were performed, as before,[10] at room temperature in a quasibackscattering geometry[11] using this time the various lines of Ar^+ and Kr^+ ion lasers, as well as a rhodomine-6G dye laser. The incident power was always 300 mW. The incident light was polarized in the scattering plane and the polarization of the scattered light was not analyzed. This

configuration corresponds closely to $z(y'y'+y'x')\bar{z}$ polarization within the sample, where z is along the [001] direction.

For backscattering at the (001) face of zinc-blende type crystals, the total Raman tensor for allowed (a) and forbidden (a_F) LO-phonon scattering is given by[12–14]

$$\overleftrightarrow{R}=\begin{bmatrix} a_F & a & 0 \\ a & a_F & 0 \\ 0 & 0 & a_F \end{bmatrix}, \tag{1}$$

where a is the sum of deformation potential and electro-optical contributions (the interband terms of the Fröhlich interaction). The electro-optical term is small for InSb.[15] The diagonal elements in Eq. (1) are due to the intraband terms of the Fröhlich interaction[12,13] or are surface field induced.[16]

The impurity-induced Raman tensor has the form[12,13]

$$\overleftrightarrow{R}_{Fi}=\begin{bmatrix} a_{Fi} & 0 & 0 \\ 0 & a_{Fi} & 0 \\ 0 & 0 & a_{Fi} \end{bmatrix}. \tag{2}$$

Earlier measurements and their analysis[12,13] have shown that most of the forbidden scattering is impurity induced even for the purest of samples.

The final result for the Raman tensor in the scattering configuration used in these experiments is

$$R_s' \propto \begin{cases} |a_F-a|^2+|a_{Fi}|^2 & \text{for } z(y'y')\bar{z}, \\ |a_F+a|^2+|a_{Fi}|^2 & \text{for } z(y'x')\bar{z}, \end{cases} \tag{3}$$

and thus contributions of all possible scattering mechanisms into the Raman intensity are expected. The tensors (1) and (2) were squared before adding terms, because the final states are different.[12,13]

The spectrometer response and other experimental corrections[17] to the measured Raman intensities were performed by the sample-substitution method[17] with pure silicon (whose susceptibility is well known[18]) as the standard. The additional correction to the alloy layer intensities for the light absorption in the top InSb layer of the superlattice structure was made using the data of Ref. 19.

III. RESULTS AND DISCUSSION

A. InSb epilayer

InSb has been amply studied by the Raman scattering method[13,14,16,20–27] and has become one of the classical materials for resonant Raman measurements.

Figure 1 shows the Raman spectrum of the InSb epilayer film. The peaks at 188 and 180 cm^{-1} are the first-order LO and transverse optical (TO) phonon modes, respectively. The latter is much weaker, because it is nearly forbidden in the experimental scattering configuration. The other features in the spectra are second order in origin.[22] The peak at 378 cm^{-1} is the first harmonic of the LO phonon, the 2LO overtone. The dependencies of the bulk-InSb LO and 2LO line intensities on the exciting light wavelength are well known from the literature[13–16,21,22] and only one RRS investigation was performed on an InSb film grown on a (001) GaAs substrate by the metalorganic magnetron sputtering technique.[27]

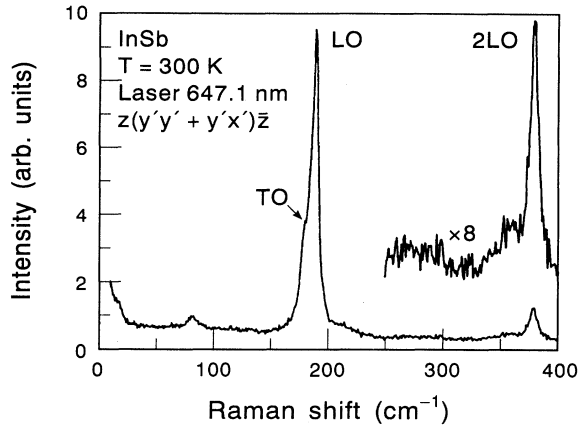

FIG. 1. Raman spectrum of the InSb epilayer recorded with 647.1 nm excitation. The spectral resolution was 2.3 cm^{-1}.

Besides the fundamental direct band gap ($E_0=0.17$ eV at room temperature[22]), InSb has a second set of direct critical points, the E_1 gap and its spin-orbit split counter-

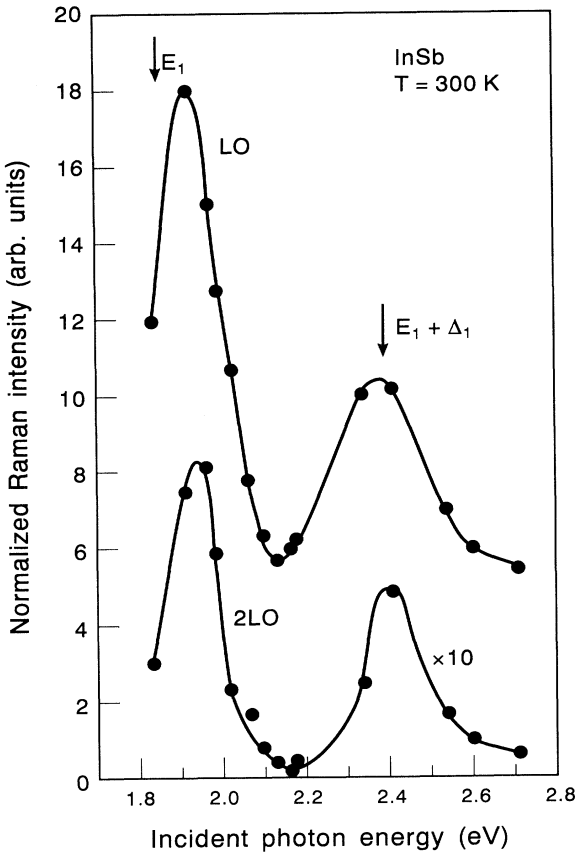

FIG. 2. Measured resonances in the Raman cross section of the InSb epilayer for LO and 2LO phonons. The arrows show the positions of the E_1 and $E_1+\Delta_1$ optical gaps found from experiment. The solid lines are guides for the eye.

part $E_1+\Delta_1$. These critical points are attributed to transitions between the upper spin-orbit-split valence and conduction bands along the $\langle 111 \rangle$ directions. The temperature dependences of the critical-point energies for bulk InSb were studied in Ref. 28. Using the values adduced in this reference and Varshni's experimental relation[29] we calculate $E_1=1.86$ eV and $E_1+\Delta_1=2.37$ eV at 300 K, which lie close to the average values $E_1=1.85$ eV and $E_1+\Delta_1=2.39$ eV determined from the various experimental measurements.[30]

The resonant behavior of the LO and 2LO phonons is shown in Fig. 2. The resonant shape is characteristic of two-band terms[17] with two peaks near E_1 and $E_1+\Delta_1$, respectively. The arrows in Fig. 2 indicate the experimental values for the critical point energies at 300 K. As in most RRS experiments, the position of the peak observed near E_1 is shifted to higher energy than the value $\hbar\omega_L=E_1+\hbar\omega_{\rm ph}/2$ expected for in-going resonance (the incident light energy $\hbar\omega_L$ equals the energy of the electronic transition) and out-going resonance (the scattered light energy equals the energy of the electronic transition) occurring together. Here, $\omega_{\rm ph}$ is the LO-phonon frequency. Such shifts, larger than $\omega_{\rm ph}/2$, are common in RRS spectroscopy and their origin is not totally understood.[17]

In so far as the small electro-optic contribution to the Raman intensity in InSb need not be taken into account,[15] the expression for the Raman polarizability associated with allowed LO scattering near the E_1 and $E_1+\Delta_1$ gaps based on the quasistatic approximation has the form[13,17]

$$a=\frac{{a_0}^2}{16\pi\sqrt{6}}\left[\frac{1}{2\sqrt{2}}d^5_{1,0}\left[\frac{E}{E_1}\frac{d\chi(E)}{dE}+\frac{\alpha}{E}\chi(E)\right]+2d^5_{3,0}\left[\frac{\chi^+(E)-\chi^-(E)}{\Delta_1}\right]+c\right], \quad (4)$$

where a_0 is the lattice constant, $d^5_{1,0}$ and $d^5_{3,0}$ are the two- and three-band deformation potentials, respectively, c is the contribution of interband transitions far from the E_1 and $E_1+\Delta_1$ gaps, and $\alpha\approx 5/2$. Equation (4) is given in terms of the following analytical expressions for the optical susceptibility χ:[13,17]

$$\chi(E)=\chi^+(E)+\chi^-(E)\ , \quad (5a)$$

$$\chi^+(E)=-\frac{A^+}{E^2}(E_1+\Delta_1/3)\ln[1-(E/E_1)^2]\ , \quad (5b)$$

$$\chi^-(E)=-\frac{A^-}{E^2}(E_1+2\Delta_1/3)\ln\{1-[E/(E_1+\Delta_1)]^2\}\ , \quad (5c)$$

where $A^+\approx A^-\approx 4\sqrt{3}\ e^2/9\pi a_0=0.54$ eV for InSb and e is the free-electron charge.

An expression similar to Eq. (4) and $\chi(E)$ obtained from ellipsometric measurements were used in fitting the RRS curves measured at low temperature in Refs. 14 and 15. There was a good coincidence of the theoretical and experimental data. Our attempt to fit the room-temperature spectral dependence of the LO-phonon RRS with Eqs. (4) and (5) and with $d^5_{1,0}=-16.2$ eV,[13] $d^5_{3,0}=32.9$ eV,[13] $A^+=0.54$ eV, and $A^-=0.49$ eV leads to agreement in the ratio of the peak intensities at the E_1 and $E_1+\Delta_1$ resonances, but the linewidth of the theoretical peaks is approximately four times narrower than the experimental ones. Thus, the broadening of the critical points with the increasing temperature[28] must be taken into account for the correct fit to the peak widths.

B. $In_{0.56}Al_{0.44}Sb$ epilayer

The existence of $In_{1-x}Al_xSb$ solid solutions over the whole composition range was shown as long ago as 1960,[31] but a Raman scattering study of this system was not carried out until now. Figure 3 shows a room-temperature Raman spectrum of the $In_{0.56}Al_{0.44}Sb$ alloy epilayer film. As expected,[10] two strong LO-phonon peaks at 183 cm^{-1} (InSb-like mode) and 306 cm^{-1} (AlSb-like mode) are observed in the spectrum. The weaker structures observed near 40, 130, and 350 cm^{-1} are second order in origin. The frequency versus concentration dependence of the AlSb-like LO mode position for bulk (fully relaxed) $In_{1-x}Al_xSb$ predicts[10] the position of the AlSb-like mode to be 312.6 cm^{-1} at $x=0.44$. The shift of this line to lower frequency in the $x=0.44$ epilayer is evidence of incomplete relaxation in the as-grown film.

The InSb-like and AlSb-like modes in Fig. 3 show resonance enhancements at exciting laser light energies of $\omega_L\approx 2.14$ eV and $\omega_L\approx 2.50$ eV (see Fig. 4) that roughly correspond to the values of the E_1 and $E_1+\Delta_1$ gap energies deduced for an $In_{0.56}Al_{0.44}Sb$ bulk sample.[32] The reasonable fits of Eqs. (4) and (5) to the experimental room-temperature spectral dependences of the InSb-like and AlSb-like LO-phonon resonance scattering are also shown in Fig. 4. Values for the deformation potentials of $d^5_{3,0}=32.9$ eV and $d^5_{1,0}=-16.2$ eV, as obtained in Ref. 13 for InSb, were used and A^+, A^-, and c were taken as

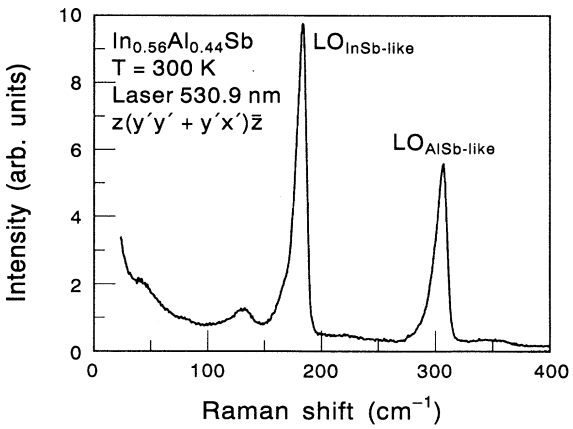

FIG. 3. Raman spectrum of the $In_{0.56}Al_{0.44}Sb$ epilayer recorded with 530.9 nm excitation. The spectral resolution was 3.5 cm^{-1}.

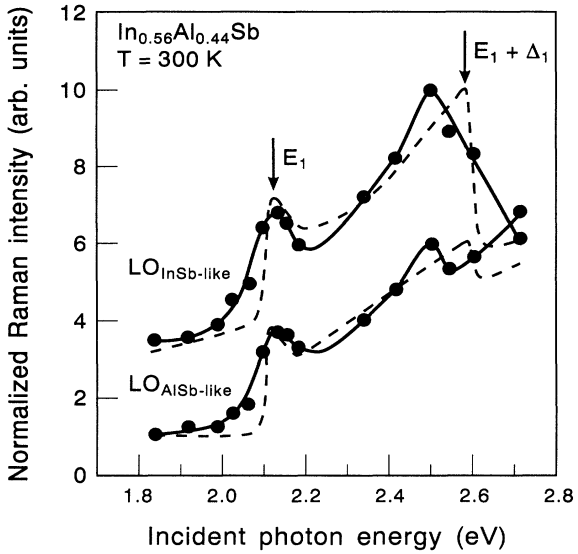

FIG. 4. Measured resonances in the Raman cross section of the $In_{0.56}Al_{0.44}Sb$ epilayer for LO InSb-like and LO AlSb-like phonons. The arrows show the positions of the E_1 and $E_1+\Delta_1$ optical gaps. The solid lines are guides for the eye. The dashed curves show the theoretical spectra calculated in the manner described in the text.

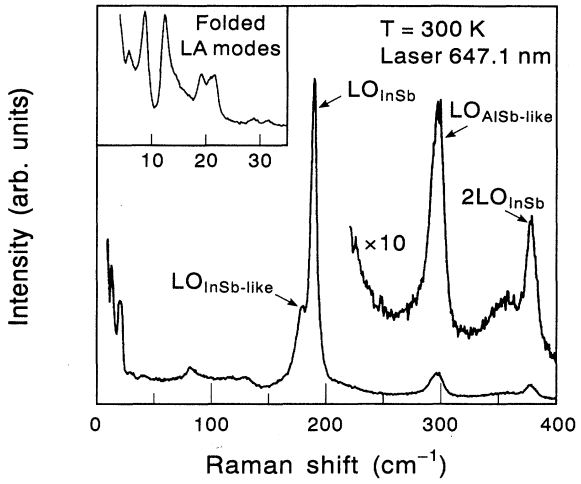

FIG. 5. Raman spectrum of the $InSb/In_{0.561}Al_{0.439}Sb$ strained-layer superlattice recorded with 647.1-nm excitation. The spectral resolution was 2.3 cm^{-1}. The inset shows a higher-resolution Raman spectrum of the folded longitudinal acoustic phonons.

fitting parameters. An important fact to be noticed is that a background with a marked dependence on the incident laser energy is present on the spectral dependencies of the LO-phonon Raman intensities in the $In_{0.56}Al_{0.44}Sb$ alloy sample. This is most obvious for the AlSb-like mode. In our opinion, the most likely explanation of this energy-dependent background is the existence of an electronic transition at higher energy. It is not possible to say more about the origin of these electronic transitions, because the electronic band structure of $In_{1-x}Al_xSb$ alloys is not known.

C. $InSb/In_{0.561}Al_{0.439}Sb$ superlattice

The Raman spectrum of the $InSb/In_{0.561}Al_{0.439}Sb$ superlattice obtained using 647.1-nm Ar^+ ion laser exciting light is shown in Fig. 5. In the frequency region shown, the spectrum exhibits sharp peaks due to LO vibrations of the InSb (labeled LO_{InSb} and $2LO_{InSb}$) and $In_{1-x}Al_xSb$ (InSb-like and AlSb-like modes labeled $LO_{InSb\text{-}like}$ and $LO_{AlSb\text{-}like}$, respectively) layers. In the low-frequency region (see inset to Fig. 5), the folded longitudinal acoustic (LA) phonons are seen.[10] The absolute and relative intensities of these modes were found to be strongly dependent on the laser excitation energy. All other weaker structures observed in the spectra are second order in origin.[22]

Figure 6 shows the resonant Raman profiles for LO and 2LO phonons of the InSb layers. The arrows indicate the positions of the respective E_1 and $E_1+\Delta_1$ peaks found in the Raman results for the InSb epilayer. The shapes and energy positions of the peaks in Fig. 6 are in good agreement with the corresponding peaks found for the InSb epilayer (see Fig. 2). The superlattice effect,

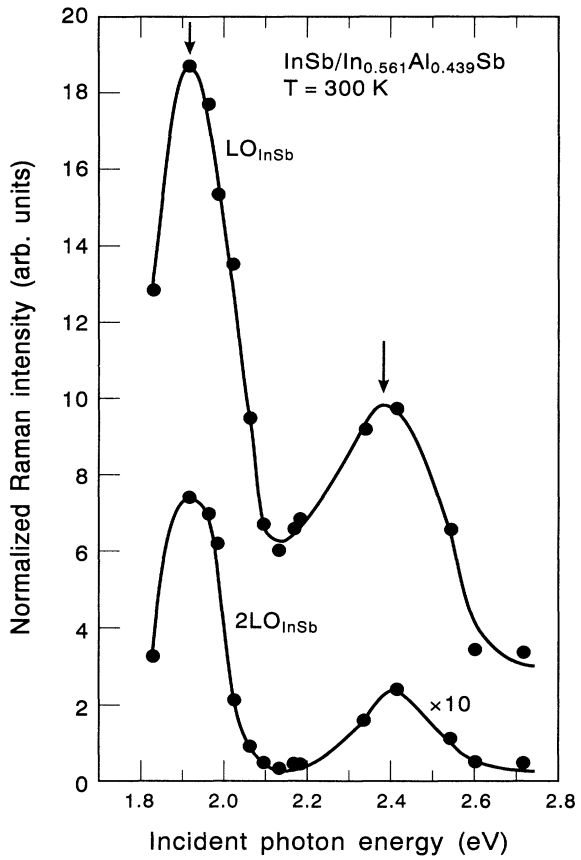

FIG. 6. Measured resonances in the Raman cross section of the $InSb/In_{0.561}$ $Al_{0.439}Sb$ superlattice for LO InSb and 2LO InSb phonons. The solid lines are guides for the eye. The arrows indicate the experimental peak positions near the E_1 and $E_1+\Delta_1$ gaps in the InSb epilayer results of Fig. 2.

which shifts the peak positions towards higher energies due to strain and confinement,[1] is thus quite small. The strain-dependent shift can be neglected for the InSb layers, as they are essentially unstrained.[10] A possible confinement effect shift is expected to be less than 0.01 eV (Ref. 7) and this small value is difficult to resolve in the room-temperature experiment.

The Raman efficiencies of the two main optical vibrations of the $In_{0.561}Al_{0.439}Sb$ alloy layer are presented in Fig. 7. In contrast to the results of Ref. 7, two weak but distinct resonant features are observed for the InSb-like mode. In addition, similar resonances are observed for the AlSb-like mode. It is also seen from Figs. 6 and 7 that the enhancements in the LO phonons originating in the alloy layers are much smaller than those for the LO phonon originating in the pure InSb layers. Peak positions in Fig. 7 are shifted to higher energy relative to the positions of the corresponding peaks of InSb in Fig. 6 by values approximately equal to the differences in the E_1 and $E_1+\Delta_1$ gaps of InSb and $In_{0.561}Al_{0.439}Sb$.[32] The observation of the separate resonant enhancements in the InSb and $In_{0.561}Al_{0.439}Sb$ layers close to the E_1 and $E_1+\Delta_1$ gap energies in the respective bulk materials means that the electronic transitions that produce the resonances in the Raman scattering are independent, or nearly independent.[1] A simple test was suggested in Ref. 33 for determination of the degree of independence of the electronic states: the ratio of the scattering intensities of the AlAs barrier modes to those of the GaAs well modes was measured. However, it is difficult to apply such a test in our case and the main reason is that the ratio of the scattering intensities of the InSb-like mode to the InSb mode is changing from ~ 1.0 to ~ 0.14 in the analyzed energy region.

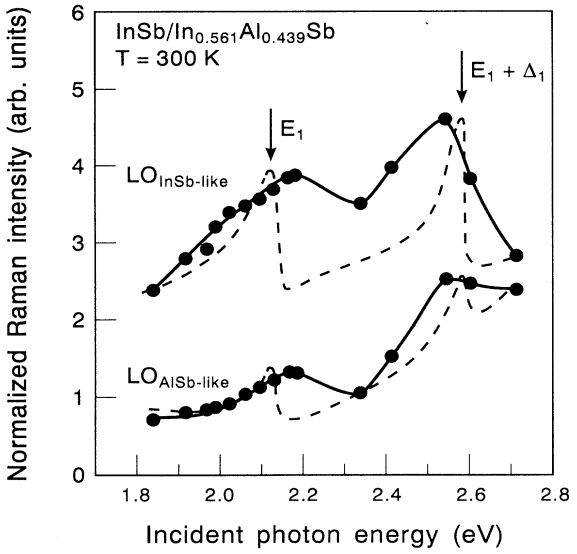

FIG. 7. Measured resonances in the Raman cross section of the $InSb/In_{0.561}Al_{0.439}Sb$ superlattice for LO InSb-like and LO AlSb-like phonons. The solid lines are guides for the eye. The arrows show the positions of the E_1 and $E_1+\Delta_1$ optical gaps in the corresponding bulk alloy material. The dashed curves show the theoretical spectra calculated using Eqs. (4) and (5). The ratio $d^5_{3,0}/d^5_{1,0}=-2$ was used and A^+, A^-, and c were taken as fitting parameters.

Figure 8 shows the resonant Raman efficiency of the InSb-like and AlSb-like optical modes of the $In_{0.56}Al_{0.44}Sb$ epilayer and $InSb/In_{0.561}Al_{0.439}Sb$ superlattice versus the energy of the incoming laser light. It seems that under resonant conditions the LO-phonon modes in the superlattice are from two to three times less intense than in the epilayer film and such behavior is apparently connected with the tensile stress in the superlattice alloy layers.[10,17] It is well known that under stress the LO-phonon scattering intensity in InSb is decreased.[34] Approximately the same ratio of intensities, as here, was observed for GaSb LO phonons in bulk material and in a GaSb/AlSb superlattice grown on (001)GaAs.[35]

The energies of resonant peaks in superlattice and bulk material are related by[7]

$$E_R(\varepsilon,d)=E_R^{\text{bulk}}+\Delta_s(\varepsilon)+\Delta_c(d)\ , \tag{6}$$

where $\Delta_s(\varepsilon)$ and $\Delta_c(d)$ are energy shifts produced by strain and confinement, respectively. The strain-induced shift is calculated to be $\Delta_s(\varepsilon)=0.043$ eV using the dependence $\Delta_s(\varepsilon)=3.016\varepsilon$ eV (Δ_s in eV) for InSb from Ref. 7 and ε evaluated from Ref. 10. The strain-induced shift is evaluated to be $\Delta_c(d)=0.011$ eV from the experimental dependence of the position of the resonant maxima (corrected for strain) versus d^{-2} for the $InSb/In_{1-x}Al_xSb$ superlattice,[7] where d is the well width. Thus, the shifts of approximately 0.05 eV (see Fig. 8) between the positions of the experimentally observed resonant peaks near the E_1 and $E_1+\Delta_1$ gap energies in the superlattice and alloy epilayer with nearly the same Al content are very close to the calculated one of $\Delta_s(\varepsilon)+\Delta_c(d)=0.054$ eV.

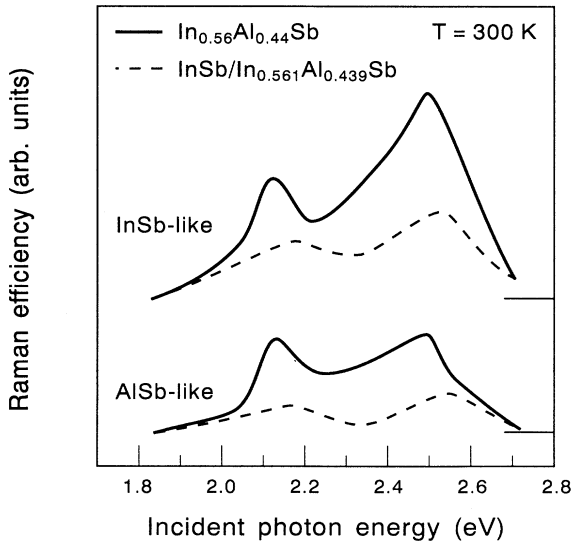

FIG. 8. Raman efficiency of LO InSb-like and AlSb-like modes of the $In_{0.56}Al_{0.44}Sb$ epilayer and the $InSb/In_{0.561}Al_{0.439}Sb$ superlattice versus the energy of the incoming laser light. The energy-dependent backgrounds have been substracted for this comparison.

IV. SUMMARY AND CONCLUSION

InSb and $In_{0.56}Al_{0.44}Sb$ epilayers and an InSb/$In_{0.561}Al_{0.439}Sb$ strained-layer superlattice have been prepared by the technique of magnetron sputter epitaxy and probed by Raman scattering spectroscopy. To our knowledge, this is the first time that the Raman scattering method has been used in the study of the $In_{1-x}Al_xSb$ alloy and only the second time in the study of the InSb/$In_{1-x}Al_xSb$ superlattice. The two-mode behavior of the $In_{1-x}Al_x$ Sb alloy phonons was clearly confirmed.

Resonant Raman experiments have allowed us to observe the spectral dependencies of the Raman cross section for LO phonons in the entire E_1 and $E_1+\Delta_1$ energy regions of InSb and $In_{0.56}Al_{0.44}Sb$. Measurements performed on the InSb/$In_{0.561}Al_{0.439}Sb$ superlattice reveal the existence of two sets of interband transitions in the regions of the E_1 and $E_1+\Delta_1$ optical gaps of the host materials. The existence of these two separate sets of resonances indicates that the electronic energy levels of the respective layers are essentially independent, i.e., the superlattice comprises a double set of multiple quantum wells for the E_1 and $E_1+\Delta_1$ transitions. By reference to the two epilayers, the resonance positions indicate that the InSb layers are not strained while the superlattice $In_{0.561}Al_{0.439}Sb$ layers are strained and the effects of both strain and confinement were evaluated.

In addition, the resonant behavior of the folded longitudinal-acoustic phonons in the superlattice was observed. Such modes are propagating through the superlattice and analysis of their resonant behavior would provide direct evidence of the degree of independence of the electronic states in the InSb/$In_{1-x}Al_xSb$ superlattice alternating layers.

ACKNOWLEDGMENT

It is a pleasure to acknowledge the technical assistance of H. J. Labbé in the Raman measurements.

*On leave from the Institute for Low Temperature Physics and Engineering of the Ukrainian Academy of Sciences, Kharkov, Ukraine.

[1]B. Jusserand and M. Cardona, in *Light Scattering in Solids V,* edited by M. Cardona and G. Güntherodt, Topics in Applied Physics Vol. 66 (Springer-Verlag, Berlin, 1989), p. 49.

[2]G. Abstreiter, E. Bauser, A. Fischer, and K. Ploog, Appl. Phys. **16**, 345 (1978).

[3]J. E. Zucker, A. Pinczuk, D. S. Chemla, A. Gossard, and W. Wiegmann, Phys. Rev. B **29**, 7065 (1984).

[4]L. Esaki, in *Proceedings of the 17th International Conference on the Physics of Semiconductors,* edited by J. D. Chadi and W. A. Harrison (Springer-Verlag, New York, 1985), p. 473.

[5]E. E. Mendez, L. L. Chang, G. Landgren, L. Ludeke, L. Esaki, and F. H. Pollak, Phys. Rev. Lett. **46**, 1230 (1981).

[6]E. E. Mendez, C. A. Chang, H. Takaoka, L. L. Chang, and L. Esaki, J. Vac. Sci. Technol. B **1**, 152 (1983).

[7]F. Cerdeira, A. Pinczuk, T. H. Chiu, and W. T. Tsang, Phys. Rev. B **32**, 1390 (1985).

[8]C. Tejedor, J. M. Calleja, F. Meseguer, E. E. Mendez, C. A. Chang, and L. Esaki, Phys. Rev. B **32**, 5303 (1985).

[9]J. B. Webb, G. H. Yousefi, and R. Rousina, Appl. Phys. Lett. **60**, 998 (1992); J. B. Webb, D. J. Lockwood, and D. Northcott, Appl. Surf. Sci. **70/71**, 526 (1993).

[10]V. P. Gnezdilov, D. J. Lockwood, and J. B. Webb, Phys. Rev. B **48**, 11 228 (1993).

[11]D. J. Lockwood, M. W. C. Dharma-wardana, J.-M. Baribeau, and D. C. Houghton, Phys. Rev. B **35**, 2243 (1987).

[12]J. Menéndez and M. Cardona, Phys. Rev. B **31**, 3696 (1985).

[13]J. Menéndez, L. Viña, M. Cardona, and E. Anastassakis, Phys. Rev. B **32**, 3966 (1985).

[14]W. Dreybrodt, W. Richter, and M. Cardona, Solid State Commun. **11**, 1127 (1972).

[15]W. Dreybrodt, W. Richter, F. Cerdeira, and M. Cardona, Phys. Status Solidi B **60**, 145 (1973).

[16]A. Pinczuk and E. Burstein, Phys. Rev. Lett. **21**, 1073 (1968).

[17]M. Cardona, in *Light Scattering in Solids II,* edited by M. Cardona and G. Güntherodt, Topics in Applied Physics Vol. 50 (Springer-Verlag, Berlin, 1982), p. 19.

[18]A. Compaan and H. J. Trodahl, Phys. Rev. B **29**, 793 (1984).

[19]O. Madelung, W. von der Osten, and U. Rössler, in *Numerical Data and Functional Relationships in Science and Technology,* edited by O. Madelung, Landolt-Börnstein, New Series, Group III, Vol. 22, Pt. a (Springer-Verlag, Berlin, 1987).

[20]R. C. C. Leite and J. F. Scott, Phys. Rev. Lett. **22**, 130 (1969).

[21]P. Y. Yu and Y. R. Shen, Phys. Rev. Lett. **29**, 468 (1972).

[22]W. Kiefer, W. Richter, and M. Cardona, Phys. Rev. B **12**, 2346 (1975).

[23]R. L. Farrow and R. K. Chang, Solid State Electron. **21**, 1347 (1978).

[24]R. Dornhaus, R. L. Farrow, and R. K. Chang, Solid State Commun. **35**, 123 (1980).

[25]K. Aoki, E. Anastassakis, and M. Cardona, Phys. Rev. B **30**, 681 (1984).

[26]E. Liarokapis and E. Anastassakis, Phys. Rev. B **30**, 2270 (1984).

[27]Z. C. Feng, S. Perkowitz, T. S. Rao, and J. B. Webb, J. Appl. Phys. **68**, 5363 (1990).

[28]S. Logothetidis, L. Viña, and M. Cardona, Phys. Rev. B **31**, 947 (1985).

[29]Y. P. Varshni, Physica (Utrecht) **34**, 149 (1967).

[30]See Refs. 2, 4, 6, 13, and 43 in Ref. 29.

[31]B. V. Baranov and N. A. Goryunova, Fiz. Tverd. Tela (Leningrad) **2**, 284 (1960) [Sov. Phys. Solid State **2**, 262 (1960)].

[32]S. Isomura, F. G. D. Prat, and J. C. Woolley, Phys. Status Solidi B **65**, 213 (1974).

[33]A. Ishibashi, M. Itabashi, Y. Mori, and N. Watanabe, Optoelectronics Dev. Technol. **1**, 51 (1986).

[34]W. Richter, R. Zeyher, and M. Cardona, Phys. Rev. B **18**, 4312 (1978).

[35]B. Jusserand, P. Voisin, M. Voos, L. L. Chang, E. E. Mendez, and L. Esaki, Appl. Phys. Lett. **46**, 678 (1985).